J Eng Math (2008) 60:101–113
DOI 10.1007/s10665-006-9135-1

Fractional-derivative viscoelastic model of the shock interaction of a rigid body with a plate

Yu. A. Rossikhin · M. V. Shitikova

Received: 27 September 2005 / Accepted: 24 December 2006 / Published online: 27 April 2007

Abstract The impact of a rigid body upon an elastic isotropic plate is investigated for the case when the equations of motion take rotary inertia and shear deformation into account. The impactor is considered as a mass point, and the contact between it and the plate is established through a buffer involving a linear-spring–fractional-derivative dashpot combination, i.e., the viscoelastic features of the buffer are described by the fractional-derivative Maxwell model. It is assumed that a transient wave of transverse shear is generated in the plate, and that the reflected wave has insufficient time to return to the location of the spring's contact with the plate before the impact process is completed. To determine the desired values behind the transverse-shear wave front, one-term ray expansions are used, as well as the equations of motion of the impactor and the contact region. As a result, we are led to a set of two linear differential equations for the displacements of the spring's upper and lower points. The solution of these equations is found analytically by the Laplace-transform method, and the time-dependence of the contact force is obtained. Numerical analysis shows that the maximum of the contact force increases, tending to the maximal contact force when the fractional parameter is equal to unity.

Keywords Fractional-derivative viscoelasticity · Ray method · Shock interaction

1 Introduction

Phillips and Calvit [1] were probably the first to investigate the response of a viscoelastic infinitely extended plate to impact of a rigid sphere. They used the Hertz's contact law in its hereditary form [2]. This problem is an immediate extension of Zener's approach [3] for the dynamic rigid spherical-indenter problem for the case of a thin elastic plate.

Yu. A. Rossikhin · M. V. Shitikova (✉)
Department of Theoretical Mechanics,
Voronezh State University of Architecture and Civil Engineering,
Svobodu Str. 45-53, Voronezh 394018, Russia
e-mail: shitikova@vmail.ru

The other approach to the problem, when viscosity is included during impact, is based on replacing Hertz's contact equation by the Maxwell equation connecting the contact force with the deformation of a viscoelastic element located between the impactor and the target. This approach was implemented by Hammel [4] for the analysis of aircraft impact on a spherical shell. The following calculation scheme has been used: an impactor moves along the normal to the shell's median surface, and a viscoelastic buffer involving an elastic spring and a dash-pot connected in series, whose one end is connected with the impactor, impacts via its other end upon the shell. Timoshenko's approach [5] was used for solving the problem in [4], since the shell was of finite dimensions. Senitskii [6] generalized Hammel's statement of the problem, taking the local bearing of the shell and the impactor materials into account. In both papers [4,5] the behavior of the shell is described by a classical set of equations.

It should be noted that linearization of the contact deformation is often used for investigating shock interactions of solids. Thus, Conway and Lee [7] considered the impact between an indenter and a large elastic plate through a linear spring, investigating the mechanics of a printing process. Qian and Swanson [8] and Chirtoforou and Swanson [9], analyzing the impact response in composite plates, used a linear spring acting between the impactor and the plate centerline deflection to represent the linearized Hertzian contact deformation. This allowed the authors to solve the problem analytically via Laplace transformation of the governing differential equations. It has been shown [10] that the use of a linear contact stiffness is useful in the identification of the key impact parameters. A comparison of this approach with the Rayleigh–Ritz technique, with finite-element calculations and experimental measurements has been carried out [8], and the range of the numerical parameters required to give good accuracy of the solution has been determined.

Problems of impact interaction of viscoelastic bodies with the use of rheological models involving fractional derivatives came under scientific scrutiny rather long ago. The first of such papers was published in 1972 by Gonsovskii et al. [11], who investigated the impact of a viscoelastic rod, the hereditary features of which were described by a fractional derivative standard linear solid model, against a rigid barrier. The rheological model was written in an equivalent form in terms of Boltzmann–Volterra relationships with a fractional exponent [12] as a weakly singular hereditary kernel. This problem was reviewed in the state-of-the-art article [13], which summed up the developments in fractional-calculus hereditary mechanics up to 1997.

Recently, interest in problems of shock interaction of viscoelastic bodies via models involving fractional derivatives and fractional integrals has been rekindled. Rossikhin and Shitikova [14] have generalized the problem [11] using the rod's model containing fractional derivatives of two different orders.

Quasi-static spherical indentation into a viscoelastic half-plane was considered in [15], wherein the shear modulus of the compressed material entering in the Hertz contact law was introduced in terms of a fractional differential operator with a time-dependent fractional parameter.

Atanackovic and Spasic [16] analyzed shock interaction of an impactor with a rigid target. The behavior of a viscoelastic buffer, clamped by its one end to the impactor, was described by a fractional-derivative standard linear solid model. The problem was reduced to investigating short-time vibrations of an oscillator occurring in a time interval equal to a half-period of vibrations, i.e., the duration of contact between the impactor and the rigid target.

Atanakovic et al. [17] investigated unilateral contact of a viscoelastic rod with a rigid wall. The rod was assumed to be massless, while the body attached to its end possessed mass. The viscoelastic properties of the rod were described by the fractional-derivative standard linear solid model. Restrictions on the model's parameters implied that the velocity after impact is smaller than before impact.

In this paper, a fractional-derivative viscoelastic model of the shock interaction of a rigid body with a plate is proposed, according to which the rigid body (impactor) impacts an upper end of a viscoelastic buffer, whose lower end is embedded into a thin body (target). As a target a non-classical plate is used, whose dynamic behavior is described by equations taking the rotary inertia and transverse shear deformations into account. The behavior of the buffer is described by the fractional-derivative Maxwell model.

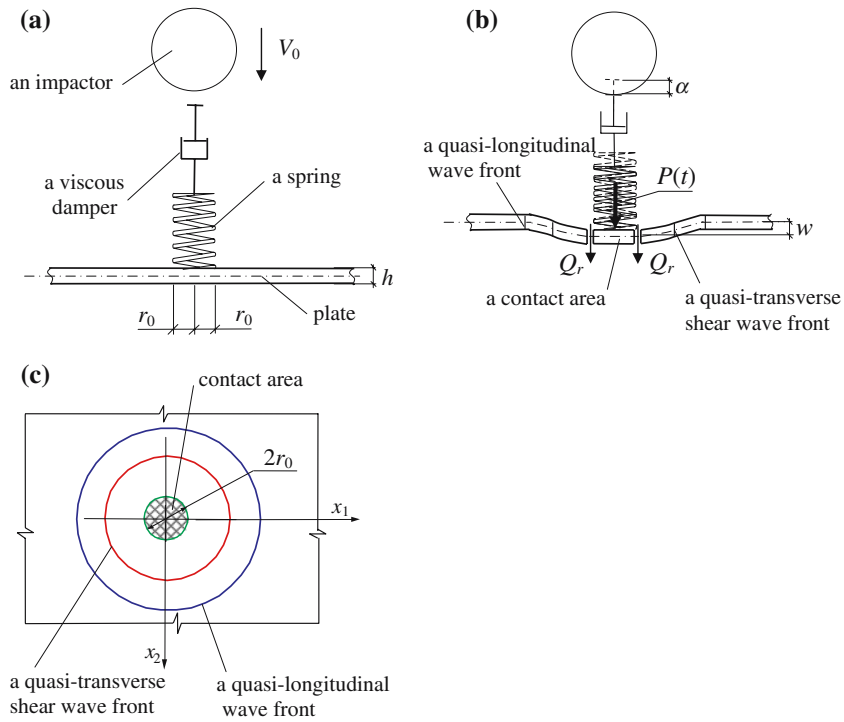

Fig. 1 Scheme of the shock interaction of a rigid body and a buffer embedded in an Uflyand–Mindlin plate. (**a**) Before interaction, (**b**) during interaction and (**c**) a plan view

2 Problem formulation and governing equations

A body with mass m moves with a velocity V_0 along the normal to the center of a circular plate and impacts upon the upper end of a viscoelastic buffer involving a viscous damper and an elastic cylindrical spring of radius r_0, which is embedded in an elastic isotropic plate of thickness h (Fig. 1). At the moment of impact, shock waves are generated in the plate, which then propagate along the plate with the velocities of transient elastic waves.

Further we shall assume that during the impact process transverse forces and transverse shear deformations predominate in the plate's stressed-deformed state in the vicinity of the contact spot (the region of plate and buffer contact). Moreover, the plate is rather wide such that reflected waves are not allowed sufficient time to return to the location of the buffer's contact with the plate before the completion of the impact process.

The behavior of a plate of the Uflyand–Mindlin type behind the fronts of the shock waves without the extension of its middle surface taken into account, is described by the following set of equations:

$$\frac{\partial Q_r}{\partial r} + \frac{1}{r} Q_r = \rho h \dot{W}, \quad \dot{Q}_r = K\mu h \left(\frac{\partial W}{\partial r} - B_r \right), \tag{1a, b}$$

$$\frac{1}{r}\left(M_r - M_\varphi\right) + \frac{\partial M_r}{\partial r} + Q_r = \frac{\rho h^3}{12} \dot{B}_r, \quad \dot{M}_r = D\left(\frac{\partial B_r}{\partial r} + \sigma \frac{B_r}{r} \right), \quad \dot{M}_\varphi = D\left(\frac{B_r}{r} + \sigma \frac{\partial B_r}{\partial r} \right), \tag{2a, b, c}$$

where r and φ are the polar radius and angle, respectively, M_r and M_φ are the bending moments, Q_r is the shear force, B_r is the angular velocity of rotation of the normal to the plate's middle surface in the r-direction, $W = \dot{w}$ is the deflection velocity, D is the cylindrical rigidity, ρ is the density, K is the shear coefficient, μ is the shear modulus, σ is Poisson's ratio, and an overdot denotes the time derivative.

The equation of motion of the impactor

$$m(\ddot{\alpha} + \ddot{w}) = -F, \tag{3}$$

and that of the contact spot (the location where, the buffer is embedded in the plate), which is considered to be a rigid body,

$$\rho h \pi r_0^2 \ddot{w} = -2\pi r_0 Q_r|_{r=r_0} + F, \tag{4}$$

where α and w are the displacements of the upper and lower points of the buffer, respectively, and F is the contact force, should be added to (1) and (2).

The contact force F is connected with the difference in displacements of the buffer's upper and lower ends by the generalized Maxwell law with the Riemann–Liouville derivative

$$F + \tau_\varepsilon^\gamma D^\gamma F = E_1 \tau_\varepsilon^\gamma D^\gamma (\alpha - w), \tag{5}$$

where τ_ε is the relaxation time, $\gamma (0 < \gamma \leq 1)$ is the fractional parameter, E_1 is the elastic coefficient of the spring, and

$$D^\gamma F = \frac{\mathrm{d}}{\mathrm{d}t} \int_0^t \frac{F\left(t - t'\right)}{\Gamma(1-\gamma)\, t'^\gamma} \mathrm{d}t'. \tag{6}$$

The initial conditions

$$\alpha|_{t=0} = w|_{t=0} = \dot{w}|_{t=0} = 0, \quad \dot{\alpha}|_{t=0} = V_0 \tag{7}$$

should be added to Eqs. 1–5.

3 Method of solution

The methods applied for solving the given problem within and outside the contact region are different. The ray method is used outside the contact spot, but the Laplace-transform method is applied within the contact region.

3.1 The ray method

Let us begin with the ray method. For this purpose, we shall interpret a shock wave in the plate (surface of strong discontinuity) as a layer of thickness δ within which the desired function Z changes from the magnitude Z^- to the magnitude Z^+ but remaining a continuous function. Then integrating (1) and (2) over the layer's thickness from $-\delta/2$ to $\delta/2$, with δ tending to zero, and considering that inside the layer the condition of compatibility [18] is fulfilled in the form of

$$\dot{Z} = -G\frac{\partial Z}{\partial r} + \frac{\delta Z}{\delta t}, \tag{8}$$

where G is the normal velocity of the wave surface, and $\delta/\delta t$ is the δ-derivative with respect to time, we find the dynamic compatibility conditions

$$[Q_r] = -\rho h G[W], \quad -G[Q_r] = K\mu h[W], \tag{9a, b}$$

$$[M_r] = -\frac{\rho h^3}{12} G[B_r], \quad -G[M_r] = D[B_r], \tag{10a, b}$$

where $[Z] = Z^+ - Z^-$.

Eliminating the values $[Q_r]$ and $[M_r]$ from (9) and (10), respectively, we define the velocities of the quasi-transverse $G^{(2)}$ and quasi-longitudinal $G^{(1)}$ waves as follows:

$$G^{(2)} = \left(\frac{K\mu}{\rho}\right)^{1/2}, \quad G^{(1)} = \left(\frac{E}{\rho(1-\sigma^2)}\right)^{1/2}, \tag{11}$$

where E is Young's modulus.

If the contact spot is considered to be a rigid body, then the values Q_r and W, which are connected by the relationship

$$Q_r = -\rho G^{(2)} h W, \tag{12}$$

are the dominating values in the vicinity of the contact spot and on its boundary.

3.2 Laplace-transform method

Substituting (12) in (4) and applying the Laplace transform to Eqs. 3 and 4 with due account for (5)–(7) yields

$$p^2 m\,(\bar{\alpha} + \bar{w}) = -\frac{(p\tau_\varepsilon)^\gamma}{1+(p\tau_\varepsilon)^\gamma} E\,(\bar{\alpha} - \bar{w}) + V_0 m, \quad Mp^2\bar{w} = -MBp\bar{w} + \frac{(p\tau_\varepsilon)^\gamma}{1+(p\tau_\varepsilon)^\gamma} E\,(\bar{\alpha} - \bar{w})\,, \tag{13a, b}$$

where p is the transform parameter, $M = \rho\pi r_0^2 h$, $\quad B = 2r_0^{-1}G^{(2)}$, and an overbar denotes the Laplace transform of the given function.

Solving (13a, b) we find

$$\bar{\alpha} = V_0 \frac{p^2 + p^{2-\gamma}\varsigma + Bp + B\varsigma p^{1-\gamma} + A}{p f_\gamma(p)}, \quad \bar{w} = V_0 \frac{A}{p f_\gamma(p)}, \tag{14a, b}$$

$$f_\gamma(p) = p^3 + p^{3-\gamma}\varsigma + Bp^2 + B\varsigma p^{2-\gamma} + Cp + BC_0, \tag{15}$$

where $\varsigma = \tau_\varepsilon^{-\gamma}$, $A = E_1 M^{-1}$, $C = E_1\left(2M^{-1} + m^{-1}\right)$, and $C_0 = E_1 m^{-1}$.

Substituting the values (14) in the expression for the contact force

$$\bar{F}(p) = \frac{(p\tau_\varepsilon)^\gamma}{1+(p\tau_\varepsilon)^\gamma} E_1(\bar{\alpha} - \bar{w}), \tag{16}$$

we have

$$\bar{F}(p) = E_1 V_0 \frac{p+B}{f_\gamma(p)}. \tag{17}$$

For $\gamma = 1$ the function $f_\gamma(p)$ in (17) should be replaced by

$$f_1(p) = p^3 + (\varsigma + B)\,p^2 + (C + B\varsigma)p + BC_0, \tag{18}$$

where $\varsigma = \tau_\varepsilon^{-1}$. In the elastic case ($\varsigma = 0$), the functions $f_\gamma(p)$ and $f_1(p)$ coincide, i.e.,

$$f_\gamma(p) = f_1(p) = p^3 + Bp^2 + Cp + BC_0. \tag{19}$$

If the impactor's mass m is far less than the mass of the contact spot M ($C \approx C_0$) or if the buffer is embedded in an absolutely rigid plate ($w = 0$), then (17) takes the form

$$\bar{F}(p) = \frac{E_1 V_0}{p^2 + \varsigma p^{2-\gamma} + C_0}. \tag{20}$$

The force $F(t)$ in the time domain is defined by the Mellin–Fourier inverse formula

$$F(t) = \frac{1}{2\pi \mathrm{i}} \int_{c-\mathrm{i}\infty}^{c+\mathrm{i}\infty} \bar{F}(p)\exp(pt)\mathrm{d}p. \tag{21}$$

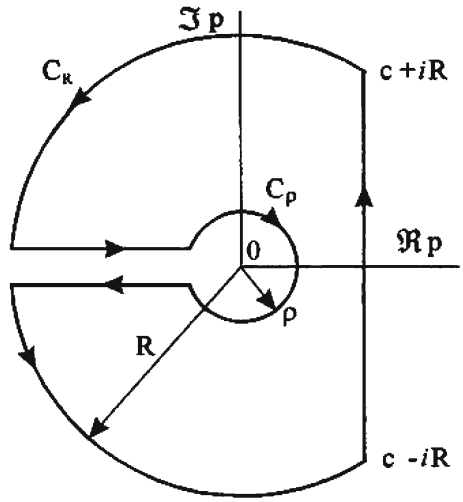

Fig. 2 Contour of integration

To calculate the integral in (21), it is necessary to determine all singular points of the complex function $\bar{F}(p)$. This function possesses the branch points $p = 0$ and $p = \infty$ and simple poles for those values of $p = p_k$ for which the denominator of (17) vanishes, i.e., which are the roots of the characteristic equation

$$f_\gamma(p) = 0. \tag{22}$$

For multivalued functions possessing branch points, the inverse theorem is valid only for the first sheet of the Riemannian surface, i.e., for $0 < |\arg p| < \pi$. Therefore the closed contour of integration should be chosen in the form shown in Fig. 2. By Jordan's lemma and application of the main theorem of the residue theory, the relationship for the contact force can be written as

$$F(t) = \frac{1}{2\pi \mathrm{i}} \int_0^\infty \left[\bar{F}\left(s\mathrm{e}^{-\mathrm{i}\pi}\right) - \bar{F}\left(s\mathrm{e}^{\mathrm{i}\pi}\right)\right] \mathrm{e}^{-st}\mathrm{d}s + \sum_k \operatorname{res}\left[\bar{F}\left(p_k\right)\mathrm{e}^{p_k t}\right], \tag{23}$$

where the summation is taken over all isolated points (poles).

It can be shown that (22) lacks real negative roots. Really, putting $p = -y$, $y > 0$, and separating real and imaginary parts, we obtain

$$-y^3 + By^2 - Cy + BC_0 - y^{3-\gamma}\varsigma\cos\pi\gamma + B\varsigma y^{2-\gamma}\cos\pi\gamma = 0, \quad y^{2-\gamma}(y - B)\varsigma\sin\pi\gamma = 0. \tag{24a, b}$$

From (24b) we find that $y = B$, and substituting the value of y obtained from (24a), we are led to the conflicting equality $B(C_0 - C) = 0$.

To find the complex conjugate roots of Eq. 22, we insert $p = r\mathrm{e}^{\mathrm{i}\psi}$ in it. Then, separating the real and imaginary parts, we obtain a set of two equations

$$r^3\left[\cos 3\psi + x\cos(3-\gamma)\psi\right] + r^2 B\left[\cos 2\psi + x\cos(2-\gamma)\psi\right] + Cr\cos\psi + BC_0 = 0, \tag{25a}$$

$$r^2\left[\sin 3\psi + x\sin(3-\gamma)\psi\right] + rB\left[\sin 2\psi + x\sin(2-\gamma)\psi\right] + C\sin\psi = 0, \tag{25b}$$

where $x = \varsigma r^{-\gamma}$.

From (25b) we find the value of r, namely

$$r = \frac{-B\left[\sin 2\psi + x\sin(2-\gamma)\psi\right] \pm \sqrt{B^2\left[\sin 2\psi + x\sin(2-\gamma)\psi\right]^2 - 4\left[\sin 3\psi + x\sin(3-\gamma)\psi\right]C\sin\psi}}{2\left[\sin 3\psi + x\sin(3-\gamma)\psi\right]}. \tag{26}$$

Then substituting r from (26) in Eq. 25a, we obtain for each fixed magnitude of the angle ψ the equation in the real positive value of x $(0 < x < \infty)$. Knowing the value of x, we define r from (26) for the same fixed

angle ψ and, finally using the connection between the values x, r and ς, we find

$$\varsigma = xr^{\gamma}. \tag{27}$$

For the characteristic equation

$$p^2 + \varsigma p^{2-\gamma} + C_0 = 0, \tag{28}$$

which enters into (20), Eqs. 25 take the form

$$r^2 \cos 2\psi + \varsigma r^{2-\gamma} \cos(2-\gamma)\,\psi + C = 0, \quad r^2 \sin 2\psi + \varsigma r^{2-\gamma} \sin(2-\gamma)\,\psi = 0. \tag{29a, b}$$

From Eqs. 29 we find for each fixed magnitude of the angle ψ

$$r^2 = C\frac{\sin(2-\gamma)\,\psi}{\sin\gamma\psi}, \quad \varsigma = -\frac{r^{\gamma}\sin 2\psi}{\sin(2-\gamma)\,\psi}. \tag{30a, b}$$

Calculations show (see Sect. 4) that both Eqs. 22 and 28 possess two complex conjugate roots for any magnitudes of γ $(0 < \gamma < 1)$ and ς $(0 < \varsigma < \infty)$.

Since the roots of the characteristic equation (22) are the complex conjugates $p = re^{\pm i\psi} = -\alpha \pm i\omega$, the relationship (23) can be written as

$$F(t) = A_0(t) + A\exp(-\alpha t)\cos(\omega t + \varphi), \tag{31}$$

where

$$A_0(t) = \frac{V_0 E_1}{\pi}\int_0^{\infty} \frac{(s-B)\Im f_{\gamma}(se^{-i\pi})e^{-st}}{\left[\Re f_{\gamma}(se^{-i\pi})\right]^2 + \left[\Im f_{\gamma}(se^{-i\pi})\right]^2}\mathrm{d}s,$$

$$\Re f_{\gamma}(se^{-i\pi}) = -s^3 - s^{3-\gamma}\varsigma\cos\pi\gamma + Bs^2 + s^{2-\gamma}B\varsigma\cos\pi\gamma - Cs + BC_0,$$

$$\Im f_{\gamma}(se^{-i\pi}) = s^{2-\gamma}\sin\pi\gamma(B-s)\varsigma,$$

$$A = \frac{2E_1V_0\sqrt{\left\{(B+r\cos\psi)\,\Re f'_{\gamma}(re^{i\psi}) + r\sin\psi\,\Im f'_{\gamma}(re^{i\psi})\right\}^2 + \left\{r\sin\psi\,\Re f'_{\gamma}(re^{i\psi}) - (B+r\cos\psi)\Im f'_{\gamma}(re^{i\psi})\right\}^2}}{\left[\Re f'_{\gamma}(re^{i\psi})\right]^2 + \left[\Im f'_{\gamma}(re^{i\psi})\right]^2}$$

$$\tan\varphi = \frac{r\sin\psi\,\Re f'_{\gamma}\left(re^{i\psi}\right) - (B + r\cos\psi)\,\Im f'_{\gamma}\left(re^{i\psi}\right)}{(B + r\cos\psi)\,\Re f'_{\gamma}\left(re^{i\psi}\right) + r\sin\psi\,\Im f'_{\gamma}\left(re^{i\psi}\right)},$$

$$\Re f'_{\gamma}\left(re^{i\psi}\right) = 3r^2\cos 2\psi + (3-\gamma)\,r^{2-\gamma}\varsigma\cos(2-\gamma)\,\psi + 2Br\cos\psi + (2-\gamma)\,B\varsigma r^{1-\gamma}\cos(1-\gamma)\,\psi + C,$$

$$\Im f'_{\gamma}\left(re^{i\psi}\right) = 3r^2\sin 2\psi + (3-\gamma)\,r^{2-\gamma}\varsigma\sin(2-\gamma)\,\psi + 2Br\sin\psi + (2-\gamma)\,B\varsigma r^{1-\gamma}\sin(1-\gamma)\,\psi.$$

The first term in (31) defines the drift of the equilibrium position, but the second describes damped vibrations around the drifting position of equilibrium. The vibratory process will cease when $F(t)$ vanishes, as the impactor then bounces back from the buffer.

When $\gamma = 1$, the first term in (31) becomes extinct, and a damping exponent, which corresponds to a real negative root of the characteristic equation

$$f_1(p) = 0, \tag{32}$$

emerges instead; in so doing, the second term remains only in the region of vibratory motions, but in the domain of aperiodic motions the sum of two damping exponents appears in its place. Therefore for $\gamma = 1$, the impactor may adhere to the buffer for certain values of τ.

Thus, for $\gamma = 1$, within the region of vibrations, we have

$$F(t) = de^{-\beta t} + A\omega^{-1}e^{-\alpha t}\sin(\omega t - \varphi), \tag{33a}$$

where $p_3 = -\beta$ is the real negative root of Eq. 32, and $p_{1,2} = -\alpha \pm \mathrm{i}\omega$ are its two complex conjugate roots,

$$d = E_1 V_0 \frac{B-\beta}{\beta^2 - 2\alpha\beta + \alpha^2 + \omega^2}, \quad A = E_1 V_0 \sqrt{a^2\omega^2 + (\alpha a - b)^2},$$
$$\tan\varphi = \frac{a\omega}{\alpha a - b}, \quad a = -d, \quad b = 1 - a\beta - 2\alpha d.$$

For $\gamma = 1$, within the region of aperiodicity, we have

$$F(t) = \left(a_1 \mathrm{e}^{-\alpha_1 t} + b_1 \mathrm{e}^{-\beta_1 t} + d_1 \mathrm{e}^{-\gamma_1 t}\right) E_1 V_0, \tag{33b}$$

where $p_1 = -\alpha_1$, $p_2 = -\beta_1$, and $p_3 = -\gamma_1$ are the real negative roots of Eq. 32,

$$a_1 = \frac{B-\alpha_1}{(\beta_1 - \alpha_1)(\gamma_1 - \alpha_1)}, \quad b_1 = \frac{B-\beta_1}{(\alpha_1 - \beta_1)(\gamma_1 - \beta_1)}, \quad d_1 = \frac{B-\gamma_1}{(\alpha_1 - \gamma_1)(\beta_1 - \gamma_1)}.$$

In the elastic case ($\varsigma = 0$), the characteristic equation,

$$p^3 + Bp^2 + Cp + BC_0 = 0, \tag{34}$$

has one real negative root $p_3 = -\beta_0$ and two purely imaginary roots $p_{1,2} = \pm \mathrm{i}\omega_0$. Therefore the expression for $F(t)$ has the form

$$F(t) = d_0 \mathrm{e}^{-\beta_0 t} + e_0 \omega_0^{-1} \sin(\omega_0 t - \varphi_0), \tag{35}$$

where $d_0 = E_1 V_0 \frac{B-\beta_0}{\beta_0^2 + \omega_0^2}$, $e_0 = E_1 V_0 \sqrt{a_0^2\omega_0^2 + b_0^2}$, $a_0 = -d_0$, and $b_0 = 1 - a_0\beta_0$.

For $C = C_0$, the roots of Eq. 34 are of the form $p_3 = -B$, $p_{1,2} = \pm \mathrm{i}\sqrt{C_0}$. If the contact force in the Laplace domain is governed by (20), then the values entering in (31) are defined in the time domain as follows

$$A_0(t) = \int_0^\infty \frac{1}{\tau} A_\varepsilon(\tau, \tau_\varepsilon)\, \mathrm{e}^{-t/\tau} \mathrm{d}\tau,$$
$$A_\varepsilon(\tau, \tau_\varepsilon) = \frac{V_0 E_1 \sin\pi\gamma}{\pi} \frac{\tau\left(1 + \tau^2 C_0\right)^{-1}}{(\tau/\tau_\varepsilon)^{-\gamma}\left(1 + \tau^2 C_0\right) + (\tau/\tau_\varepsilon)^{\gamma}\left(1 + \tau^2 C_0\right)^{-1} + 2\cos\pi\gamma}, \tag{36}$$
$$A = E_1 V_0 r^{-1}\left[4 + \varsigma^2 (2-\gamma)^2 r^{-2\gamma} + 4 r^{-\gamma} \varsigma (2-\gamma)\cos\gamma\psi\right]^{-1/2},$$
$$\tan\varphi = -\frac{2r\sin\psi + \varsigma(2-\gamma) r^{1-\gamma}\sin(1-\gamma)\psi}{2r\cos\psi + \varsigma(2-\gamma) r^{1-\gamma}\cos(1-\gamma)\psi}.$$

4 Numerical analysis

As an example, consider the impact of rigid body (Fig. 1) moving with a velocity $V_0 = 10\,\mathrm{m/s}$ at the moment of impact upon a plate of thickness $h = 0.1\,\mathrm{m}$ with the embedded buffer having a radius $r_0 = 0.1\,\mathrm{m}$ and the spring's rigidity being $E_1 = 252.53\,\mathrm{kN/m}$. The material of the plate possesses the following characteristics: $E = 200\,\mathrm{GPa}$, $\sigma = 0.3$, and $\rho = 7850\,\mathrm{kg/m^3}$.

To investigate the ς-dependence of the behavior of the roots of Eqs. 22 and 28, let us reduce it to dimensionless form, respectively, as

$$f_\gamma^*(p^*) = p^{*3} + \varsigma(BC_0)^{-\gamma/3}(p^*)^{3-\gamma} + B^{2/3}C_0^{-1/3}p^{*2} + \varsigma(BC_0)^{(2-\gamma)/3}(p^*)^{2-\gamma} + C(BC_0)^{-2/3}p^* + 1 = 0, \tag{37}$$

where $p^* = p(BC_0)^{-1/3}$, and

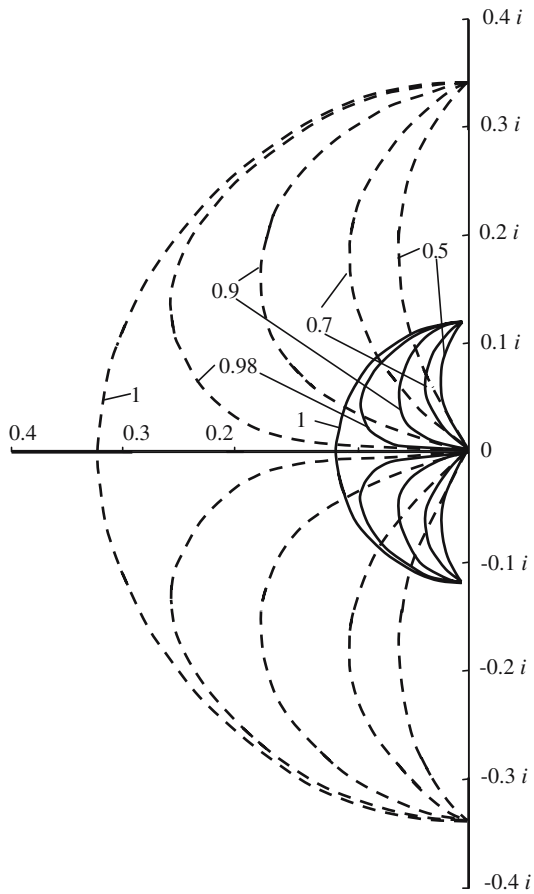

Fig. 3 Roots of the characteristic equations: _ _ _ _ _ Eq. 38, _____ Eq. 37

$$f_\gamma^*(p^*) = p^{*2} + \varsigma C_0^{-\gamma/2}(p^*)^{2-\gamma} + 1 = 0, \tag{38}$$

where $p^* = pC_0^{-1/2}$.

As has been shown above, these equations possess only two complex conjugate roots for $\gamma \neq 1$ and $\varsigma \neq 0$, whose behavior as a function of the parameter ς is presented in the complex plane p^* (see Fig. 3) for the following values: $C/C_0 = 1$ (dashed lines) and $C/C_0 = 41.55$ (solid lines). The values of the parameter γ are indicated by numbers near the curves. It is seen that, for $C = C_0$, all the roots of (38) emanate from 0 for $\varsigma = \infty$ and for $\varsigma = 0$ come to the points that are aligned with the imaginary axis. For $C \neq C_0$ all roots emanate from 0 for $\varsigma = \infty$ and for $\varsigma = 0$ come to the points that are not aligned with the imaginary axis, but are the complex roots of Eq. 37. Reference to Fig. 3 shows also that, for $\gamma \neq 1$, the roots of these characteristic equations do not intersect the real negative semi-axis for any values of the parameter ς, i.e., for $\gamma \neq 1$ these equations lack the domain of aperiodicity. For $\gamma = 1$ two complex conjugate roots intersect the real negative semi-axis and, starting from this value of ς, this characteristic equation possesses three real negative roots that govern the aperiodic motion of the system, resulting in an infinitely large duration of the contact between the impactor and the buffer. When $C \to C_0$, solid lines go over into the corresponding dashed lines.

The time-dependence of the contact force is shown for $C = C_0$ and $C \neq C_0$, respectively, in Figs. 4 and 5, which corresponds to an impactor's mass of 1 and 500 kg, respectively, for the following values of the fractional parameter: $\gamma = 1$ (Figs. 4a and 5a), $\gamma = 0.9$ (Figs. 4b and 5b), $\gamma = 0.7$ (Figs. 4c and 5c), and $\gamma = 0.5$ (Figs. 4d and 5d). The values of the relaxation time τ_ε are indicated in the figure captions. It is seen that, for each fixed value of γ, the maximum of the contact force decreases when the

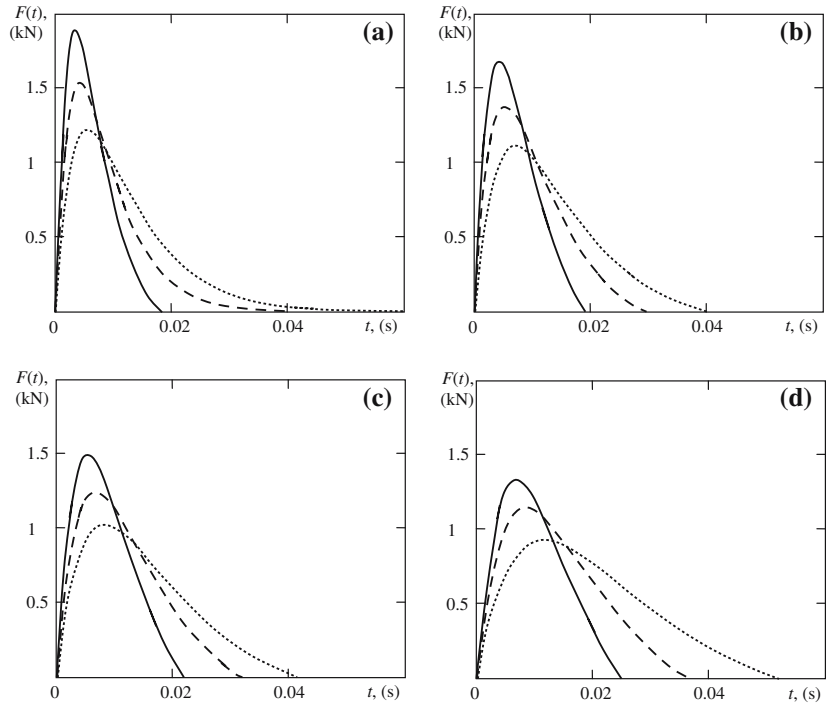

Fig. 4 The time dependence of the contact force for $C = C_0$ for fixed values of the fractional parameter: (**a**) $\gamma = 1$, (**b**) $\gamma = 0.9$, (**c**) $\gamma = 0.7$, and (**d**) $\gamma = 0.5$, $\tau_\varepsilon = 0.002\,\mathrm{s}$ —, $\tau_\varepsilon = 0.001\,\mathrm{s}$ – – – –, $\tau_\varepsilon = 0.0001\,\mathrm{s}$ .....

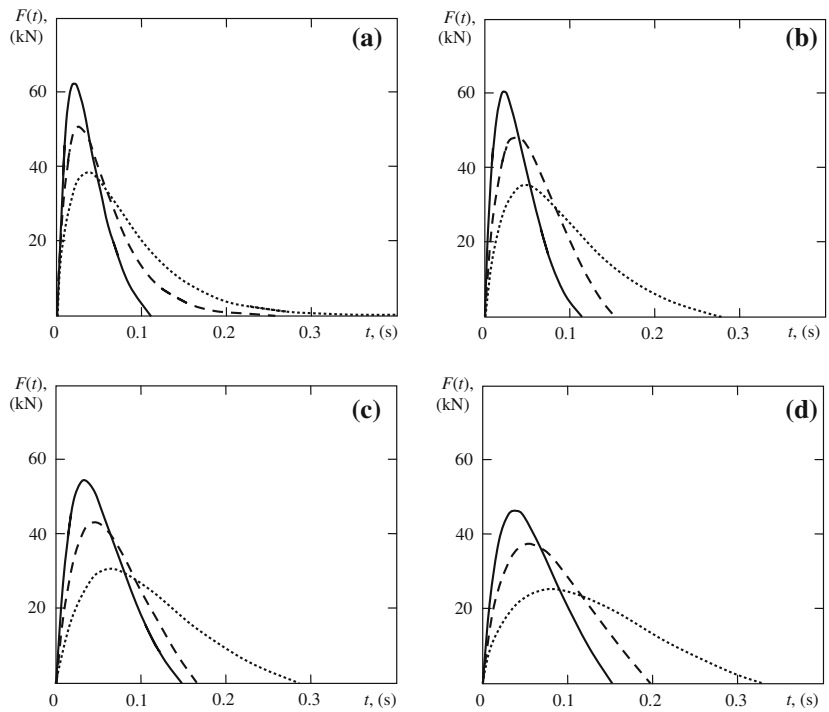

Fig. 5 The time dependence of the contact force for $C \neq C_0$ for fixed values of the fractional parameter: (**a**) $\gamma = 1$, (**b**) $\gamma = 0.9$, (c) $\gamma = 0.7$, and (d) $\gamma = 0.5$, $\tau_\varepsilon = 0.035\,\mathrm{s}$ —, $\tau_\varepsilon = 0.023\,\mathrm{s}$ – – – –, $\tau_\varepsilon = 0.015\,\mathrm{s}$ .....

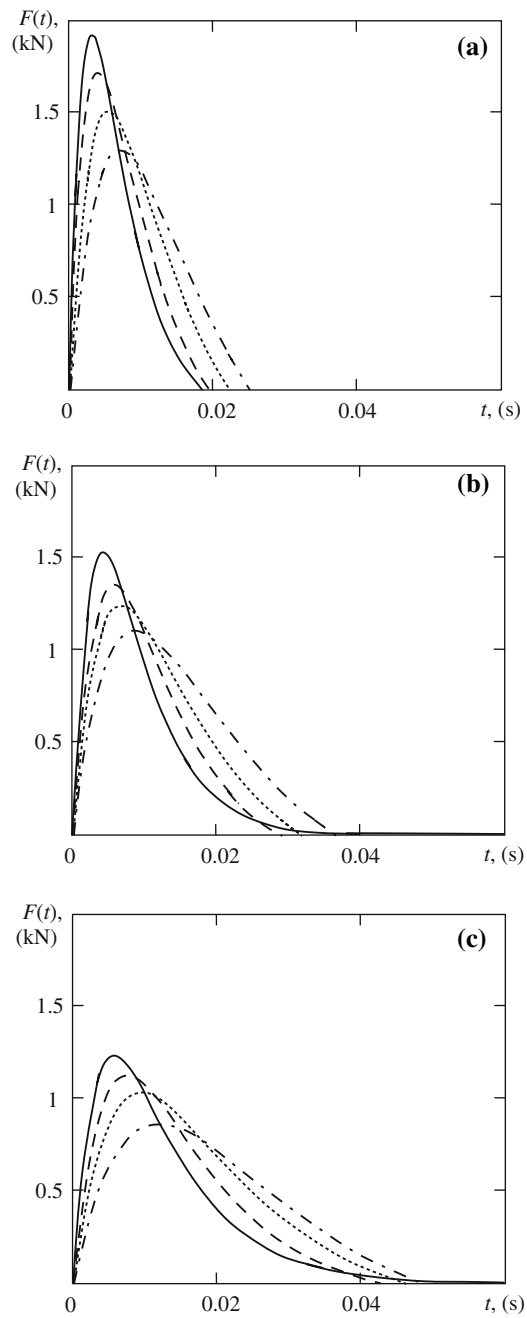

Fig. 6 The time dependence of the contact force for $C = C_0$ for fixed values of the relaxation time: (**a**) $\tau_\varepsilon = 0.002$ s, (**b**) $\tau_\varepsilon = 0.001$ s, and (**c**) $\tau_\varepsilon = 0.0001$ s, $\gamma = 1$ —, $\gamma = 09$ - - - -, $\gamma = 0.7$ ....., $\gamma = 0.5$ -. -. -.

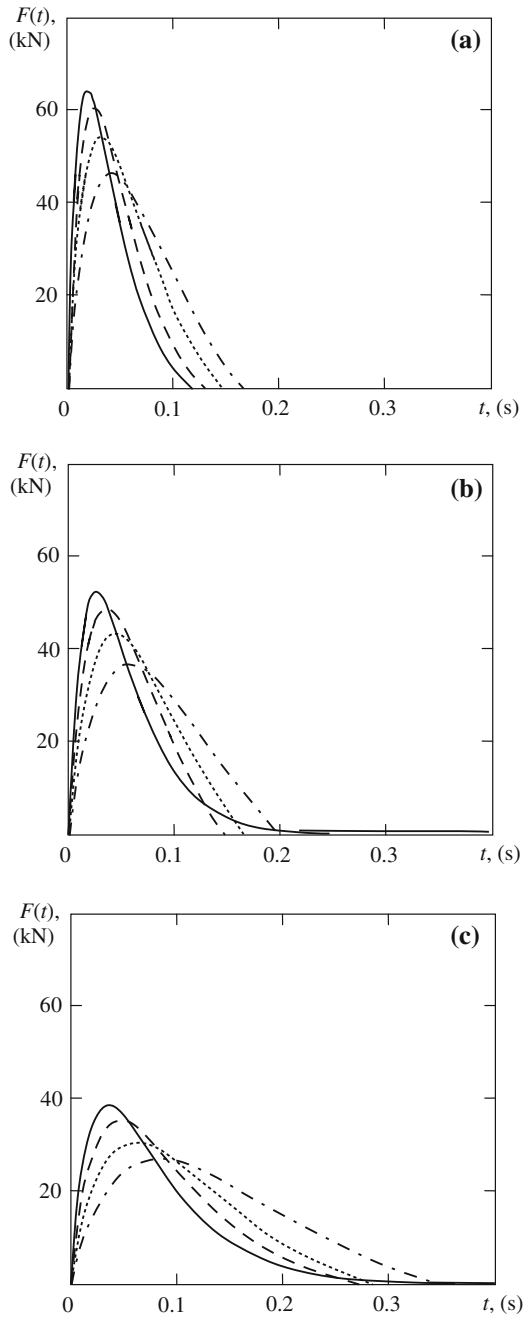

Fig. 7 The time dependence of the contact force for $C \neq C_0$ for fixed values of the relaxation time: (**a**) $\tau_\varepsilon = 0.002$ s, (**b**) $\tau_\varepsilon = 0.001$ s, and (**c**) $\tau_\varepsilon = 0.0001$ s, $\gamma = 1$ —, $\gamma = 0.9$ - - - - , $\gamma = 0.7$ ....., $\gamma = 0.5$ -. -. -. -.

relaxation time decrease, but the duration of contact increases. Starting from a value $\tau_\varepsilon = 0.001$ s in the case of $C = C_0$ and $\tau_\varepsilon = 0.023$ in the case of $C \neq C_0$, respectively, the contact duration becomes infinitely large.

Table 1 The rebound velocity of the sphere V^* depending on the relaxation time τ_ε and the fractional parameter γ for $m = 1$ kg

τ_ε	γ			
	1.0	0.9	0.7	0.5
2×10^{-3}	1.9	2.3	2.5	3.0
1×10^{-3}	2.5	3.5	4.0	4.5
1×10^{-4}	3.75	4.5	5.0	6.25

Table 2 The rebound velocity of the sphere V^* depending on the relaxation time τ_ε and the fractional parameter γ for $m = 500$ kg

τ_ε	γ			
	1.0	0.9	0.7	0.5
2×10^{-3}	1.81	2.1	2.4	2.8
1×10^{-3}	2.05	2.18	2.63	2.92
1×10^{-4}	2.2	2.4	2.8	3.1

Figures 6 and 7 show the time-dependence of the contact force for $C = C_0$ and $C \neq C_0$, respectively, for fixed values of the parameter τ_ε, while the fractional parameter γ plays the role of a variable. A comparison of the curves depicted in Figs. 6 and 7 shows that all curves experience "smearing" when the fractional parameter γ is decreased, i.e., its value influences both the maximal magnitude of the contact force and the contact duration. As this takes place, when $\gamma \neq 1$, the duration of contact remains finite for any value of τ_ε.

When Figs. 4 and 5 are compared with Figs. 6 and 7, it is clear that the relaxation time and the fractional parameter have the same influence on the behavior of the curves for the time dependence of the contact force.

Reference to Figs. 4–7 shows that the contact duration is of the order of 10^{-2} s (Figs. 4 and 6) or 10^{-1} s (Figs. 5 and 7) depending on an impactor mass of $m = 1$ kg or $m = 500$ kg, respectively.

When the duration of contact t^* between the sphere and the plate is known, it is possible to determine the velocity V^* at the end of impact, i.e., at the moment when the sphere bounces back off the plate. Integrating (3) with respect to t from 0 to t^* yields

$$V^* = V_0 - \frac{1}{m}\int_0^{t^*} F(t)\mathrm{d}t. \tag{39}$$

Equation 39 allows one to obtain the relaxation time τ_ε and the dependence of the rebound velocity V^* on the fractional-parameter γ; this is illustrated in Tables 1 and 2 using data presented in Figs. 6 and 7.

Reference to Tables 1 and 2 shows that a decrease in the relaxation time for fixed values of the fractional parameter γ results in an increase of the velocity V^* at the end of impact; a decrease in the fractional parameter γ for fixed values of τ_ε also causes V^* to increase. In other words, the smaller the fractional parameter γ is, the smaller the energy dissipation occurring during the process of impact will be. The reason is that for $\gamma \to 0$ the viscoelastic rheological model (5) goes over into an elastic model.

5 Conclusions

The problem considered here admits a more general treatment than the impact of a body upon a spring with a damper embedded in a plate. This problem concerns the shock interaction of the impactor and the target, wherein the generalized Maxwell law instead of the Hertz contact law is employed as a law of interaction. Two parameters appear in this law: the relaxation time τ_ε and the fractional parameter γ that can be varied in order to match the theoretical results with experimental data.

It has been shown that both parameters affect the maximum value of the contact force and the contact duration, namely: an increase in the parameters τ_ε and γ results in a decrease of the maximum of the contact force and in an increase in the contact duration. However, irrespective of τ_ε, whose variation is

primarily connected with a change in time, the variation of γ has other causes: X-ray radiation, electromagnetic fields, and so on; for examples see [13]. Thus, the parameter γ could be considered as the structural parameter responding to changes in the structure of the material on a molecular level.

The contact force is defined by two processes: the relaxation and the inertial processes. The first term in Eq. 31 describes predominantly the relaxation process, while the second governs essentially the inertial process. The character of the behavior of the contact force with time depends on the dominant factor in the process. Due to the relaxation process, all curves depicting the time-dependence of the contact force experience "smearing" with a decrease in the fractional parameter γ, i.e., its value influences both the maximum value of the contact force and the contact duration. As this takes place, when $\gamma \neq 1$, the duration of contact remains finite for any values of τ_ε.

Numerical investigation shows that the velocity of the impactor after impact is smaller than the velocity before impact which is consistent with the physical nature of the interaction process under investigation. As this takes place, a decrease in the relaxation time for a fixed value of the fractional parameter results in an increase of the velocity at the end of impact, and a decrease in the fractional parameter for fixed values of the relaxation time also causes the velocity at the moment of rebound to increase. In other words, the smaller the fractional parameter is, the smaller the energy dissipation occurring during the impact process will be. The reason is that for $\gamma \to 0$ the rheological viscoelastic fractional-derivative model under consideration goes over into an elastic model.

Acknowledgments The research described in this paper has been made possible in part by the Russian Foundation for Basic Research under grant no. 05-08-17936.

References

1. Phillips JW, Calvit HH (1967) Impact of a rigid sphere on a viscoelastic plate. ASME J Appl Mech 34:873–878
2. Hunter SC (1960) The Hertz problem for a rigid spherical indenter and a viscoelastic half space. J Mech Phys Solids 8:219–234
3. Zener C (1941) The intrinsic inelasticity of large plates. Phys Rev 59:669–673
4. Hammel J (1976) Aircraft impact on a spherical shell. Nuclear Eng Design 37:205–223
5. Timoshenko SP (1914) Zur Frage nach der Wirkung eines Strosse anf einer Balken. Z Math Phys 62:198–209
6. Senitskii YuE (1982) Impact of a viscoelastic solid along a shallow spherical shell. Mech Solids (Engl. trans.) 17:120–124
7. Conway HD, Lee HC (1970) Impact of an indenter on a large plate. ASME J Appl Mech 37:234–235
8. Qian Y, Swanson SR (1990) A comparison of solution techniques for impact response of composite plates. Compos Struct 14:177–192
9. Christoforou AP, Swanson SR (1991) Analysis of impact response in composite plates. Int J Solids Struct 27: 161–170
10. Christoforou AP, Yigit AS (1998) Effect of flexibility on low velocity impact response. J Sound Vibr 217:563–578
11. Gonsovskii VL, Meshkov SI, Rossikhin YuA (1972) Impact of a viscoelastic rod onto rigid target. Int Appl Mech (Engl. trans.) 8:1109–1113
12. Rabotnov YuN (1948) Equilibrium of an elastic medium with after-effect (Russian). Prikl Mat Mekh 12:53–62
13. Rossikhin YuA, Shitikova MV (1997) Application of fractional calculus to dynamic problems of linear and nonlinear hereditary mechanics of solids. Appl Mech Rev 50:15–67
14. Rossikhin YuA, Shitikova MV (2001) Analysis of dynamic behaviour of viscoelastic rods whose rheological models contain fractional derivatives of two different orders. ZAMM 81:363–376
15. Ingman D, Suzdalnitsky J, Zeifman M (2000) Constitutive dynamic-order model for nonlinear contact phenomena. ASME J Appl Mech 67:383–390
16. Atanackovic TM, Spasic DT (2004) On viscoelastic compliant contact-impact models. ASME J Appl Mech 71:134–138
17. Atanackovic TM, Oparnica L, Pilipovic S (2006) On a model of viscoelastic rod in unilateral contact with a rigid wall. IMA J Appl Math 71:1–13
18. Rossikhin YuA, Shitikova MV (1995) The ray method for solving boundary problems of wave dynamics for bodies having curvilinear anisotropy. Acta Mech 109:49–64